Quench and Normal Zone Propagation Characteristics of RHQT-Processed Nb_3Al Wires Under Cryocooler-Cooling Conditions

Satoru Murase, M. Shimoyama, N. Nanato, S. B. Kim, G. Nishijima, K. Watanabe, A. Kikuchi, N. Banno, and T. Takeuchi

***Abstract*—The minimum quench energy (MQE) and normal zone propagation velocity ($NZPV$) of three kinds of Nb_3Al superconductors fabricated by the rapid heating, quenching and transformation (RHQT) process were measured under various conditions of applied magnetic field (10–14 T), temperature (7–11 K), and transport current (80–95% of the critical current), while cooled by a cryocooler for developing the over 20-T class cryogen-free magnet. As a result, MQE values were related to the critical current density (J_c); high MQE was obtained for low J_c. It is assumed that J_c has a stronger influence on the MQE than specific heat, thermal conductivity, resistivity, and other parameters of the composite superconductor including the matrix and the stabilizer. $NZPV$ was mainly proportional to the transport current density varying with applied field and temperature. The second contribution to $NZPV$ is assumed to be heat capacity depending on the wire configuration.**

***Index Terms*—Cryocooler cooling, Nb_3Al, superconducting wire, thermal stability.**

I. Introduction

RECENTLY, a cryocooler-cooled superconducting magnet has progressed with developments of 4K-cryocooler and power lead made by high temperature superconductor (HTSC). An over 20-T cryocooler-cooled magnet has been designed for demands of higher magnetic fields as described in [1]. To fabricate those high-field magnets, it is essential to understand the thermal stability of the superconducting wires under the cryocooler-cooling. However, while a lot of studies concerned with stability under the pool-boiling cooling condition have been achieved, such as Maddock's equal area theory [2], Stekly's classic cryostatic stability criterion [3], and CCM stability criterion [4], fewer have addressed stability under the cryocooler-cooling conditions.

Previously, there were some reports on thermal stability of Nb_3Sn wires under pulsed and external-oriented disturbances caused by wire-movements and cracks in epoxy in the potted coil under cryocooler-cooling conditions [5]–[8]. In these cases, the minimum quench energy (MQE) behavior was characterized by only one empirical equation [8].

Nb_3Al has advantages of better strain tolerance over Nb_3Sn [9]. The RHQT (Rapid, Heating, Quenching and Transformation)-processed Nb_3Al wires, in particular, have high critical current density, J_c, (e.g. over 1,000 A/mm^2 at 4.2 and 16 T) and are one of the most promising wires [9]. Nb_3Al wires have different component materials from Nb_3Sn wires; the matrices are Ta and/or Nb for Nb_3Al and Cu-Sn for Nb_3Sn. Those differences affect the thermal stability, the MQE and the normal zone propagation velocity ($NZPV$).

In this paper we study and discuss the thermal stability of three types of RHQT-processed Nb_3Al wires under cryocooler-cooling conditions.

II. Experimental Procedure

A. Sample Preparation

Three types, nos. 1, 2 and 3, of RHQT-processed Nb_3Al wires were fabricated for stability measurements [10], [11]. They have a Cu external stabilizer of 45.8%–50% in the volume fraction. In no. 3 sample Ta and Nb were used for the inter-filament matrix and for the outer-most matrix, respectively. The Cu stabilizer was electroplated with a high velocity (5 m per hour) after 1 μm-ion-plating. An argon-ion bombardment carried out prior to copper ion-plating yields a good contact between Cu and Nb. In no. 1 sample Nb was used for both of the inter-filament and the outer-most matrix. The Cu electroplating with slow velocity and the ion-plating process were also used for the stabilizer fabricating. In no. 2 sample Nb for the inter-filament barrier and Ta for the outermost and the center-core were used. The Cu stabilizer was mechanically clad. The specifications of those sample wires are shown in Table I.

B. Basic Properties Measurements

In the experiment, the sample wire was wound around a FRP (Fiber-Reinforcement-Plastic; G-10) bobbin with a 36 mm diameter. The sample wire was wound in the groove on the

Manuscript received August 16, 2008. First published June 30, 2009; current version published July 15, 2009. This work was supported in part by the Budget of the National Institute for Materials Science and the Budget for Nuclear Research of the Ministry of Education, Culture, Sports, Science and Technology, based on the screening and counseling by the Atomic Energy Commission. Part of this work was performed at High Field Laboratory for Superconducting Materials, Institute for Material Research, Tohoku University.

S. Murase, M. Shimoyama, N. Nanato and S. B. Kim are with the Department of Electrical and Electronic Engineering, Okayama University, 3-1-1, Tsushimanaka, Okayama 700-8530, Japan (e-mail: murase@elec.okayama-u.ac.jp).

G. Nishijima and K. Watanabe are with the HFLSM, Institute for Material Research, Tohoku University, 2-2-1 Katahira, Aobo-ku, Sendai 980-8577, Japan.

A. Kikuchi, N. Banno and T. Takeuchi are with the National Institute for Materials Science, 1-2-1, Sengen, Tsukuba 305-0047, Japan.

Color versions of one or more of the figures in this paper are available online at http://ieeexplore.ieee.org.

Digital Object Identifier 10.1109/TASC.2009.2018149

TABLE I
SPECIFICATION OF Nb3Al SAMPLES

Sample ID	No. 1	No. 2	No. 3
Strand Diameter (mm)	1	1	1
Matrix Material			
Inter-filament	Nb	Nb	Ta
Outermost	Nb	Ta	Nb
Center Core	Nb	Ta	Ta
Filament Diameter (μm)	50	7.6	38
No. of Filaments	144	66 x 54	222
Volume Fraction of Cu (%)	50	45.8	50

FRP bobbin and fixed with grease. Both ends of the wire were connected to the current terminals cooled by the cryocooler. The sample bobbin was installed on the second stage of a GM-cryocooler, which was able to control the temperature from 4 K to approximately 40 K. For applying the magnetic field the sample stage was installed into the cryogen-free superconducting magnet, 15T-CSM, in the Institute for Materials Research, Tohoku University. Voltage taps and temperature measuring sensors (Cernox) were set on the sample. Signals obtained from them were recorded by a personal computer and a digital oscilloscope [5]–[8]. The critical temperature (T_c) was measured by the resistance method in accordance with the international standards of T_c measurement method, IEC 61788-10, in changing the temperature using the cryocooler under applied magnetic fields. Based on the T_c measurement standard the transport current was 1 A. The critical current (I_c) was measured at temperatures from 7 K to 11 K and at applied magnetic fields from 10 T to 14 T, using a 100 $\mu V/m$ criterion. The critical current density (J_c) was defined as I_c divided by the cross-sectional area of non-copper.

C. Stability Measurements

The sample was installed in the same way as the basic properties measurement. Furthermore, a 1.5-mm square thin strain gauge was used for generating the heat disturbance, which was put on the sample. Disturbance energy increased by a 0.06-mJ step was inputted to the sample under a transport current of 80 % to 95 % of I_c. In increasing of the stepped input energy, the minimum energy that causes quench of the sample wire was defined as the minimum quench energy, MQE. The MQE measurements were performed at applied magnetic fields of 10 T–14 T, at temperatures of 8 K–11 K and the normalized transport current (defined as transport current divided by I_c). The normal zone generated by the heat disturbance was detected by the voltage taps and the travel time of the normal zone from one voltage tap to next one was measured. The normal zone propagation velocity $(NZPV)$ was determined as the traveling velocity of the normal zone from one voltage tap to another. These thermal stability properties were measured with changing temperatures and applied magnetic fields.

III. RESULTS AND DISCUSSIONS

A. T_c and J_c

Critical temperatures versus applied magnetic fields for nos. 2 and 3 are shown in Fig. 1. They show almost the same results. J_c versus temperature at 14 T for nos. 1, 2 and 3 are shown in Fig. 2. The J_c of no. 2 sample is lower than those of nos. 1 and 3. No. 2 sample has the same T_c as no. 3 but lower J_c. Since the filament array of no. 2 is the double stack structure, it increases the matrix ratio against the Nb_3Al superconducting filaments. The non-copper J_c of no. 2 is believed to be lowered by the filament structure although the intrinsic J_c values are almost the same.

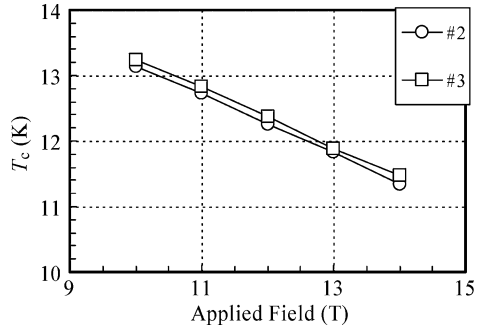

Fig. 1. Critical temperature (T_c) as a function of applied magnetic field for nos. 2 and 3.

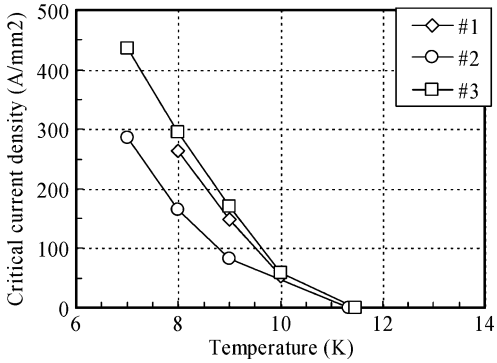

Fig. 2. Critical current density at 14 T as a function of temperature for nos. 1, 2 and 3.

B. MQE Properties

We obtained a lot of data about MQE properties in various conditions of applied magnetic field, temperature and transport current. MQE characteristics of no. 2 sample with the highest MQE are reported. MQE against the normalized transport current in various applied fields from 10 T to 14 T at 8 K and in various temperatures from 8 K to 11 K at 10 T are shown in Figs. 3 and 4, respectively. As the normalized transport current (the loaded current) and the applied magnetic field increased, the MQE decreased. The typical results of MQE characteristics in the cryocooler cooling, i.e. MQE decrease with increase of fields, were observed because the MQE in the cryocooler cooling is determined by the temperature margin [5]–[8]. It is different from MQE characteristics in the immersed cooling using the cryogen; i.e. MQE increase with increase of fields, because Joule heating is dominant. The temperature dependence of the MQE is also explained by the temperature margin stability.

The loaded-current dependence of the MQE at 14 T and 9 K for three types of samples, nos. 1, 2 and 3, is shown in Fig. 5. All samples reveal that the MQE decreases with the increase of

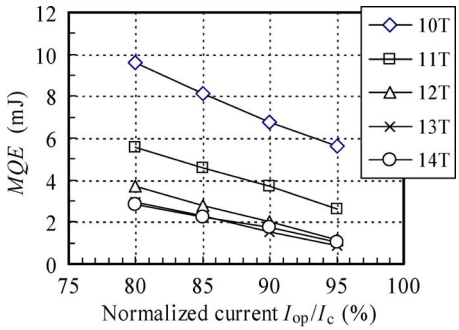

Fig. 3. MQE as a function of normalized current at 8 K in 10 T–14 T for no. 2.

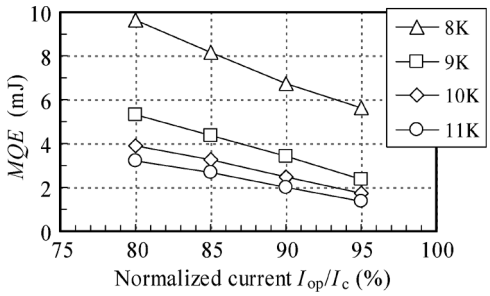

Fig. 4. MQE as a function of normalized current at 10 T in 8 K–11 K for no. 2.

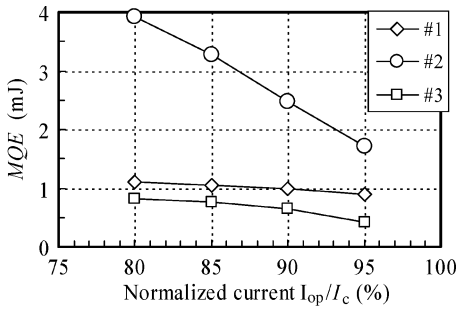

Fig. 5. MQE as a function of normalized current at 14 T and 9 K for nos. 1, 2 and 3.

the loaded-current, and MQE values of nos. 1 and 3 are smaller than those of no. 2. As pointed out in sub-clause A, J_c values of no. 2 are smaller than those of nos. 1 and 3; high MQE is obtained for low J_c. It is considered that the wire has large tolerance against quench in the case of low J_c that does not bring about high energy when the quench occurred. As shown in Figs. 3, 4 and 5, the MQEs could not approach zero at the normalized current of 1 by using a linear extrapolation. One of the reasons may be that the I_c criterion of 100 μV/m is not enough for quench, and a 10 μV/m criterion that is hard to be measured in the measurement apparatus. Another reason is that linear relationship between MQE and the normalized current may not show at around 100% of the normalized current.

C. $NZPV$ Properties

The dependence of transport current density (J_{op}) for the no. 3 sample on $NZPV$ at 9 K in 11 T–14 T is shown in Fig. 6 as one of the typical $NZPV$ characteristics. The $NZPV$ increased with an increase of J_{op}. Since the magnetic field

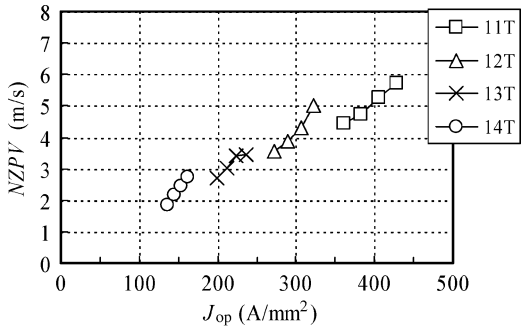

Fig. 6. $NZPV$ as a function of J_{op} at 9 K in 11 T–14 T for no. 3.

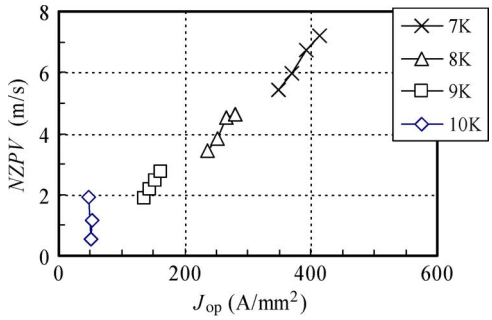

Fig. 7. $NZPV$ as a function of J_{op} at 14 T in 7 K–10 K for no. 3.

increased, J_c and J_{op} decreased and therefore the $NZPV$ decreased. Furthermore, the dependence of J_{op} for no. 3 on $NZPV$ at 14 T in 7 K–10 K is shown in Fig. 7. As the temperature increased, J_c and J_{op} also decreased, therefore the $NZPV$ decreased. Specifically, the $NZPV$ diminished with increasing of magnetic fields and temperatures. In other words, the $NZPV$ has an approximately linear relation with J_{op}. An $NZPV$ equation is given in (1) under pool-boiling conditions. Variables "y" and "z" are defined by a steady-state term (2) and a transient term (3), respectively [12].

$$NZPV = \frac{J_{op}}{\gamma c}\left(\frac{\rho\kappa}{T_c - T_{op}}\right)^{\frac{1}{2}} \frac{(1-2y)}{(yz^2+z+1-y)^{\frac{1}{2}}} \quad (1)$$

$$y = \frac{hP(T_c - T_{op})}{AJ_{op}^2\rho} \quad (2)$$

$$z = \frac{Q_L}{\gamma C(T_c - T_{op})} \quad (3)$$

Here, γ, C, A, κ, and ρ, are volume heat capacity, cross-sectional area, thermal conductivity and resistivity of the wire, respectively. P, Q_L, h and T_{op} present a cooling perimeter, a latent heat, a heat transfer coefficient, the operation temperature, respectively. In the cryocooler-cooling condition the term "y" is considered to be very small. According to (1), although the $NZPV$ varies roughly linearly with J_{op} when the temperature and the magnetic field are constant, the vicinity of $J_{op} = 0$ is not defined. Consequently, as shown in Figs. 6, 7, and 8, the $NZPV$s could not approach zero at $J_{op} = 0$ by a linear extrapolation. In the case of the temperature change, as shown in Fig. 7, thermal conductivity, resistivity and heat capacity also vary. In (1) "$\rho\kappa$" is almost constant obeying Wiedemann-Frantz

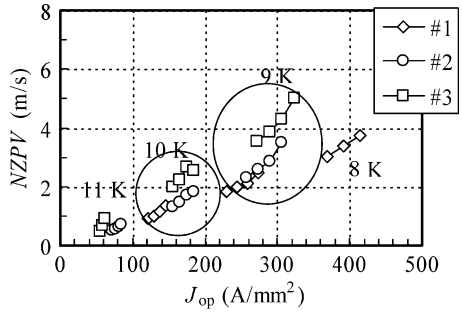

Fig. 8. $NZPV$ as a function of J_{op} at 12 T in 8 K–11 K for nos. 1, 2 and 3.

rule, but the heat capacity increases with almost T^3. Therefore, $NZPV$ at low temperature is slower than that at high temperature.

$NZPV$ vs. J_{op} characteristics for three kinds of Nb_3Al wires at 12 T in temperatures from 8 K to 11 K are shown in Fig. 8. Although it is difficult to compare them at the same conditions for J_{op}, magnetic fields and temperatures, it is observed that the $NZPV$ of no. 3 is larger than those of no. 1 and no. 2. It is known that the volume specific heat of Ta is smaller than that of Nb [13]. As shown in Table I, the volume fraction of Ta for no. 3 is larger than that for nos. 1 and 2. It is assumed that the wire with large Ta volume fraction has large $NZPV$ as obtained from (1).

IV. Conclusions

MQE and $NZPV$, thermal stabilities, of three kinds of Nb_3Al superconductors by the RHQT process were measured under various conditions of the applied magnetic field, temperature, and the transport current cooled by the 4K cryocooler. Obtained significant knowledge is as follows;

1) MQE values related to the J_c; high MQE was obtained for low J_c. It is assumed that J_c has stronger influence on the MQE than specific heat, thermal conductivity, resistivity, and other parameters of the composite superconductor including the matrix and the stabilizer.
2) $NZPV$ was mainly proportional to the transport current density varying with applied fields and temperatures.

The second contribution to $NZPV$ is assumed to be heat capacity depending on the wire configuration.

References

[1] K. Watanabe, S. Awaji, G. Nishijima, T. Hamajima, T. Kiyoshi, H. Kumakura, S. Hanai, and M. Ono, "Case study of a 20 T- φ400 mm room temperature bore superconducting outsert for a 45 T hybrid magnet," *IEEE. Trans. Appl. Supercond.*, vol. 18, pp. 552–555, June 2008.

[2] B. J. Maddock, G. B. James, and W. T. Norris, "Superconductive composites: Heat transfer and steady state stabilization," *Cryogenics*, vol. 9, pp. 261–273, 1969.

[3] A. R. Kantrowitz and Z. J. J. Stekly, "A new principle for the construction of stabilized superconducting coils," *Appl. Phys. Letters*, vol. 6, pp. 56–57, Feb. 1965.

[4] Y. Iwasa, "A critical current-margin design criterion for high performance magnet stability," *Cryogenics*, vol. 19, pp. 705–714, 1979.

[5] T. Kaneko, T. Seto, T. Nanbu, S. Murase, S. Shimamoto, S. Awaji, K. Watanabe, M. Motokawa, and T. Saito, "Stability of Nb_3Sn wires with CuNb reinforcing stabilizer on cryocooled superconducting magnet," *IEEE Trans. Appl. Supercond.*, vol. 10, pp. 1235–1238, 2000.

[6] S. Murase, T. Murakami, T. Seto, S. Shimamoto, S. Awaji, K. Watanabe, T. Saito, G. Iwaki, and S. Meguro, "Normal zone propagation of Nb_3Sn wires with jelly-roll and in-situ processed CuNb reinforcements," *IEEE Trans. Appl. Supercond.*, vol. 11, no. 1, pp. 3627–3630, 2000.

[7] T. Yamamoto, K. Watanabe, S. Murase, G. Nishijima, K. Watanabe, and A. Kimura, "Thermal stability of reinforced Nb_3Sn composite superconductor under cryocooled conditions," *Cryogenics*, vol. 44, pp. 687–693, 2004.

[8] K. Watanabe, T. Mitsuhashi, N. Nanato, S. Kim, S. Murase, G. Nishijima, K. Watanabe, and K. Miyoshi, "Effects of Cu stabilizer configuration on thermal stability of Nb_3Sn composite superconductors under cryocooling condition," *IEEE Trans. Appl. Supercond.*, vol. 15, pp. 3410–3413, June 2005.

[9] T. Takeuchi, " Nb_3Al conductors for high-field applications," *Supercond. Sci. Technol.*, vol. 13, pp. R101–R109, 2000.

[10] A. Kikuchi, R. Yamada, E. Barzi, M. Lamm, T. Takeuchi, D. Turrioni, A. V. Zlobin, and B. Smith, "Cu stabilized Nb_3Al strands for the high field accelerator magnet," *IEEE. Trans. Appl. Supercond.*, vol. 18, pp. 1026–1030, June 2008.

[11] N. Banno, T. Takeuchi, Y. Iijima, A. Kikuchi, and K. Tagawa, "Reduction of the matrix ratio for improvement of the non-Cu Jc of Nb3Al wires," *IEEE. Trans. Appl. Supercond.*, vol. 18, pp. 1035–1038, June 2008.

[12] M. N. Wilson, *Superconducting Magnets*. New York: Oxford University Press, 1983.

[13] W. Wasserbach, S. Abens, and S. Sahling, "Low-temperature thermal conductivity and specific heat of plastically deformed high-purity tantalum single crystals," *J. Low Temp. Phys.*, vol. 123, pp. 251–274, 2001.